Archives of Acoustics Vol. 46, No. 4, pp. 667–675 (2021), doi: 10.24425/aoa.2021.139643

Research Paper

Experimental Determination of a Reflective Muffler Scattering Matrix for Single-Mode Excitation

Łukasz GORAZD

AGH University of Science and Technology, Faculty of Mechanical Engineering and Robotics
Krakow, Poland; e-mail: lukasz.gorazd@agh.edu.pl

(*received May 20, 2021; accepted July 1, 2021*)

The aim of the paper is to experimentally determine the scattering matrix **S** of an example reflective muffler of cylindrical geometry for Helmholtz number exceeding the plane wave propagation.

Determining the scattering matrix of an acoustic systems is a new and increasingly used approach in the assessment of reduction of noise propagating inside duct-like elements of heating, ventilation and air conditioning systems (HVAC). The scattering matrix of an acoustic system provides all necessary information on the propagation of wave through it. In case of the analysed reflective silencer, considered as a two-port system, the noise reduction was determined by calculating the transmission loss parameter (TL) based on the scattering matrix (**S**). Measurements were carried out in two planes of the cross-section of pipes connected to the muffler.

The paper presents results of the scattering matrix evaluation for the wave composed of the plane wave (mode (0,0)) and the first radial mode (0,1), each of which was generated separately using the self-designed and constructed single-mode generator. The gain of proceeding measurements for single modes stems from the fact that theoretically, calculation of the **S**-matrix does not require, as will be presented in the paper, calculation of the measurement data inverse matrix. Moreover, if single mode sound fields are well determined, it ensures error minimization. The presented measurement results refer to an example of a duct like system with a reflective muffler for which the scattering matrix **S** was determined. The acoustic phenomena inside such a system can be scaled by the parameter *ka*.

Keywords: cylindrical duct; reflective muffler; single-mode generation; multi-port method; scattering matrix.

1. Introduction

Waveguides are structures inside which an acoustic wave propagates efficiently, i.e. without significant loss of energy. They can be found in heating, ventilation and air conditioning (HVAC) systems, which outlets are sources of industrial noise of high levels. That is why techniques leading to reduction of this unwanted and environmentally harmful noise have been receiving much attention. This resulted in new methods of theoretical analysis such as multi-port method (Sack *et al.*, 2016) and more and more advanced constructions of noise attenuating devices (Snakowska, Jurkiewicz, 2021) together with application of new materials such as acoustical metamaterials (Auregan *et al.*, 2016).

Acoustic mufflers are systems most frequently used to reduce the excessive sound level emitted to the environment through their outlets. According to the method of attenuating acoustic waves, mufflers can be divided into reflective and absorption mufflers. The type of muffler used depends, inter alia, on the required frequency band to be attenuated as well as the pollution conditions of the medium flowing through the waveguide. It is also possible to use combinations of different types of mufflers to achieve the desired effect. Reflective mufflers operate on the principle of reflection and interference of acoustic waves due to the inclusion of discontinuities (junctions) in the duct introducing change of the acoustic impedance on both sides of the discontinuity. To meet nowadays expectations on environmental noise protection, the muffler design has become more and more complicated, to mention only mufflers consisting of several chambers (multi-chamber muffler) (Munjal, 1987), with extended chamber inlet/outlet pipe (Munjal, 1987) or by-pass elements (Snakowska, Jurkiewicz, 2021) which incorporated

into the system change phase of the propagating wave as in Herschel-Quincke tube (Salamet *et al.*, 1994).

Propagation of sound in duct-like systems comprises also radiation of environmental harmful sound through outlets of jet engines, compressors, stacks etc. Depending on the level of complication of the physical system, different methods are applied to analyse the sound field radiated from the outlet, starting from theoretical solutions derived for example for radiation from the outlet of a hard-walled flanged or unflanged duct (Hocter, 2000; Joseph, Morfey, 1999; Sinayoko *et al.*, 2010; Snakowska, Jurkiewicz, 2010; Zorumski, 1973) through numerical methods of Computational Aero-Acoustics (CAA) (Hocter, 1999; Chen *et al.*, 2004; Lidoine *et al.*, 2001; Atig *et al.*, 2004; Dalmont *et al.*, 2001) up to Computational Fluid Mechanics (CFD) (Su *et al.*, 2015) applied to radiation from complex-shape outlets of turbofan engines.

In theoretical analysis applied to mufflers, it is often assumed that only a plane wave propagates through the system and that the approach based on continuity of the volume velocity is justified (Munjal, 1987). Then the most frequently applied method is the transfer matrix method (Song, Bolton, 2000; Gerges *et al.*, 2005).

In fact, both of these assumptions can lead to significant errors even in the range of frequencies for which only the plane wave can propagate without attenuation, namely when the Helmholtz number (in literature called also reduced frequency or dimensionless frequency) ka ($k = \omega/c$ – wave number, ω – angular frequency, c – sound speed, and a – duct radius) does not exceed the cut-on frequency of the first Bessel mode, which is 3.83 for the first radial mode (0,1) and 1.84 for the first circumferential mode (1,1). The sources of errors in this approach stems from the fact that such approach does not account for the phenomena (such as mode transformation) which assure fulfilment of the boundary condition (Snakowska, Jurkiewicz, 2021) at junctions of pipes of different cross-sections. Another reason can be weak attenuation of the first Bessel mode for frequencies close to its cut-on frequency. Furthermore, this approach becomes incorrect for Helmholtz numbers exceeding the before mentioned cut-on reduced frequency in any sub-system of a muffler.

As we can see, in the case of a multimode wave, the description of phenomena inside a waveguide with incorporated muffler becomes much more complicated but can be efficiently analysed by means of the multi-port method.

The one-, two-, and multi-port methods have been presented in many papers (Sack *et al.*, 2016; Snakowska, Jurkiewicz, 2021; Lavrentjev *et al.*, 1995; Abom, Karlsson, 2010). In general, the n-port method ($n = 1, 2, 3...$) can be developed based on a number of different formulations depending on the choice of two state variables, which could be: the acoustic pressure p, the acoustic velocity v or the acoustic pressures p^+, p^- of waves travelling across a joint in both directions. It leads to the transmission (**T**), the impedance (**Z**) or the scattering (**S**) matrix approach.

To describe how a muffler reduces the sound level of an N-mode wave we have to determine any of these matrices exciting N substantially different sound fields. The most general method, applicable not only in cascade-like shape of a muffler, is the scattering matrix method, which is applied in this paper. It is relatively new but more and more frequently used approach in the assessment of noise reduction inside elements of ventilation and air-conditioning system, such as waveguides with reflective mufflers (Abom, 1991).

The scattering matrix of an acoustic system provides all necessary information on the propagation of wave through it. In case of mufflers, it allows to determine reduction of noise by calculating such parameters as the transmission loss (TL) or the insertion loss (IL).

The efficient method leading to the results is the multi-port method according to which the considered system constitutes a two-port. Experimental determination of the scattering matrix of a two-port requires measurements executed at each port that is on both sides of the muffler in two planes of the cross-section of pipes connected to the muffler (Sitel *et al.*, 2006).

The paper presents results of the scattering matrix evaluation for the wave composed of the plane wave (mode (0,0)) and the first radial mode (0,1), each of which was generated separately. The measurements were carried out by means of the self-designed single mode generator (Snakowska *et al.*, 2016) containing a matrix of point sources excited with separate loudspeakers.

The gain of generating "pure" single mode stems from the fact that in such case calculation of the **S**-matrix does not require, as will be presented in the paper, calculation of the inverse matrix of experimental data. In practice, mode selected to be generated is always accompanied by other modes (Snakowska *et al.*, 2016), however of much lower amplitudes and so exited fields are substantially different and the matrix of experimental data is well determined. It is important as in general the **S**-matrix determination represents an inverse problem.

In Sec. 2 the multi-port method and basic assumptions are described in short, together with its main theoretical formulae. Section 3 justifies application of the scattering matrix method comparing it to other formalisms such as the transmission and impedance matrix methods. Section 4 contains descriptions of the experimental measurements, the most important parameters of the measurement set-up and measurement data. Section 5 presents final result of the **S**-matrix determination and TL calculation.

2. The multi-port method and basic assumptions

Theoretical considerations are related to the propagation of sound in a rigid cylindrical duct corresponding to the mathematical model of a waveguide in which normal component of the acoustic velocity $v_n = 0$ on its surface, i.e. Neumann's boundary condition for the acoustic pressure (Munjal, 1987). Geometry of the system is presented in Fig. 1. It consists of an inlet/outlet pipe connected to a segment of a larger radius pipe chamber. The inlet/outlet pipes are long enough to apply the two-port method. The main assumptions of this method and applied definition of an n-port are as stated below and follow the approach presented in the paper on the theory of multi-ports network applied to muffler analysis (Snakowska, Jurkiewicz, 2021).

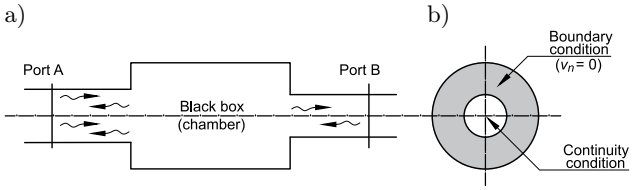

Fig. 1. Sketch of the a) two-port system, b) cross-section of the junction.

An acoustic multi-port is defined by the number of pipes connected to the considered element (subsystem), independently on sizes of different ducts and the frequency of excitation. This approach is in agreement with the topology of the system (Snakowska, Jurkiewicz, 2021). In the two-port method the system presented in Fig. 1 will be described as composed of two joints (inlet and outlet pipes) and a "black box" (chamber). The main assumptions of the method applicability are: the sound pressure wave in joints can be decomposed into wave going in and out of the "black box" and represented by a superposition of duct modes. Modes amplitudes at a given duct cross-section can be presented as one-column matrices. It is very important that joints are long enough to consider only the propagating waves at selected cross sections called ports. This allows to neglect cut-off modes exited at junction to ensure continuity of the acoustic pressure and the normal velocity (at common surface of both pipes) together with compliance of the boundary condition (at rigid surface of larger pipe), as presented in Fig. 1b.

In what follows mathematical formulae will be presented for cylindrical symmetry as a muffler of such symmetry and will be analysed here after, however the method can be applied also to duct-like systems of other geometries, such as cartesian or elliptical.

To determine amplitudes of individual modes of wave propagating through the system the modal decomposition was performed using Fourier-Lommel transform (Auger, Ville, 1990). In general, assuming a certain sound source operating inside the system, radial and circumferential modes are exited, however due to system axial symmetry only radial modes ($m = 0$) will be considered in the final formulae only. The time factor is assumed in the form $e^{i\omega t}$ and is omitted throughout the text.

Total acoustic pressure is a sum of contributions coming from individual cut-on modes:

$$p(\rho,\varphi,z) = \sum_{m,l} p_{m,l}(\rho,\varphi,z), \tag{1}$$

while the acoustic pressure of a single mode decomposed into $p^{+}_{ml}(\rho,\varphi,z)$ and $p^{-}_{ml}(\rho,\varphi,z)$ in perfectly hard-walled cylindrical waveguide is described by the formulae

$$p_{ml}(\rho,\varphi,z) = p^{+}_{ml}(\rho,\varphi,z) + p^{-}_{ml}(\rho,\varphi,z), \tag{2}$$

$$p^{\pm}_{ml}(\rho,\varphi,z) = P^{\pm}_{ml}\psi_{ml}(\rho,\varphi)e^{\pm ik_{z,ml}z}, \tag{3}$$

$$\psi_{ml}(\rho,\varphi) = \Lambda_{ml}e^{im\varphi}J_m\left(\mu_{ml}\frac{\rho}{a}\right), \tag{4}$$

where $p^{\pm}_{ml}$ is the acoustic pressure of the (ml) ingoing/out-going mode, $P^{\pm}_{ml}$ is the amplitude of the mode, $k_{z,ml}$ is the axial wave number, ψ_{ml} is the mode shape function, Λ_{ml} is the modal normalization constant, $J_m(x)$ is the Bessel function of first kind, and μ_{ml}/a is the radial wave number fulfilling in a duct of radius a boundary condition $J'_m(\mu_{ml}) = 0$.

3. The scattering matrix method compared to other formalisms

To describe the sound pressure field of the wave propagating inside the duct-like system along the z-axis (which is the duct axis), one of the following formalisms can be used depending on choice of state variables. The selection of the state variables as $\mathbf{P}_A = \mathbf{P}(z_1)$, $\mathbf{V}_A = \mathbf{V}(z_1)$ and $\mathbf{P}_B = \mathbf{P}(z_2)$, $\mathbf{V}_B = \mathbf{V}(z_2)$ (that is acoustic one-column matrices of modes velocity and pressure amplitudes at points z_1 and z_2) leads to the most commonly used formalism of the transfer matrix $\mathbf{T}$, but also to the impedance $\mathbf{Z}$ and admittance matrix $\mathbf{Y} = \mathbf{Z}^{-1}$ being the inverse of the impedance matrix $\mathbf{Z}$

$$\begin{bmatrix}\mathbf{P}_B\\ \mathbf{V}_B\end{bmatrix} = \begin{bmatrix}\mathbf{T}^{11} & \mathbf{T}^{12}\\ \mathbf{T}^{21} & \mathbf{T}^{22}\end{bmatrix}\times\begin{bmatrix}\mathbf{P}_A\\ \mathbf{V}_A\end{bmatrix}, \tag{5}$$

$$\begin{bmatrix}\mathbf{P}_A\\ \mathbf{P}_B\end{bmatrix} = \begin{bmatrix}\mathbf{Z}^{11} & \mathbf{Z}^{12}\\ \mathbf{Z}^{21} & \mathbf{Z}^{22}\end{bmatrix}\times\begin{bmatrix}\mathbf{V}_A\\ \mathbf{V}_B\end{bmatrix}, \tag{6}$$

$$\begin{bmatrix}\mathbf{V}_A\\ \mathbf{V}_B\end{bmatrix} = \begin{bmatrix}\mathbf{Y}^{11} & \mathbf{Y}^{12}\\ \mathbf{Y}^{21} & \mathbf{Y}^{22}\end{bmatrix}\times\begin{bmatrix}\mathbf{P}_A\\ \mathbf{P}_B\end{bmatrix}. \tag{7}$$

Each of these formalisms has some pros and cons. For example, the transfer matrix ($\mathbf{T}$) formalism is commonly used in cascade-like systems, but cannot be used

for multi-ports other than two-ports (for example for a "black box" connected to more than two pipes) as well as to describe phenomena occurring at the waveguide outlet – acoustic one port (Snakowska *et al.*, 2017). The experimental determination of the scattering matrix **S** requires more extensive measurement set up in relation to the transition matrix **T**, while application of the scattering matrix formalism is the most general and can be used in single-, two- and in general multi-ports, while the transfer matrix formalism only in two-ports.

The selection of the state variables $\mathbf{P}^{\text{in}}$, $\mathbf{P}^{\text{out}}$ that is modal pressure amplitudes of waves in-going to and out-going from the "black box" (sub-system of unknown acoustical properties) through joints to selected ports A (at z_1) and B (at z_2), leads to the formalism of the scattering matrix **S**. Thus, elements of a given column of the **S**-matrix indicate how the amplitude of the selected in-going pressure mode is distributed between the modes out-going through all joints (more precisely – ports at all joints), whereas elements of a given row describe contribution of all in-going modes to a selected out-going mode. Thus, the **S**-matrix elements represent the mode reflection/transformation coefficients and the transmission coefficients. For that reason, for total number N_{tot} of modes in-going through all joints the **S**-matrix dimension is $2N_{\text{tot}} \times 2N_{\text{tot}}$.

The wave propagating along each joint may consist of different number of modes, depending on its size. Equations (8)–(11) present the two-port method and the **S**-matrix formalism matrices of in-going and out-going pressure modes, assuming that N_A and N_B modes propagate through joints A and B, respectively. Moreover, to avoid four indices in **S** matrix elements (contribution of mode (ml) to mode (ml)) mode single indexing was introduced, which is a common practice

$$\begin{aligned}\mathbf{P}^{\text{in},A} &= \begin{bmatrix} P_1^{\text{in},A} \\ \vdots \\ P_N^{\text{in},A} \end{bmatrix} \mathbf{P}^{\text{out},A} = \begin{bmatrix} P_1^{\text{out},A} \\ \vdots \\ P_N^{\text{out},A} \end{bmatrix} \mathbf{P}^{\text{out},B} \\ &= \begin{bmatrix} P_1^{\text{out},B} \\ \vdots \\ P_N^{\text{out},B} \end{bmatrix} \mathbf{P}^{\text{in},B} = \begin{bmatrix} P_1^{\text{in},B} \\ \vdots \\ P_N^{\text{in},B} \end{bmatrix}, \end{aligned} \tag{8}$$

$$\mathbf{P}^{\text{in}} = \begin{bmatrix} \mathbf{P}^{\text{in},A} \\ \mathbf{P}^{\text{in},B} \end{bmatrix} \mathbf{P}^{\text{out}} = \begin{bmatrix} \mathbf{P}^{\text{out},A} \\ \mathbf{P}^{\text{out},B} \end{bmatrix}, \tag{9}$$

$$\begin{bmatrix} \mathbf{P}^{\text{out},A} \\ \mathbf{P}^{\text{out},B} \end{bmatrix} = \begin{bmatrix} \mathbf{S}^{11} & \mathbf{S}^{12} \\ \mathbf{S}^{21} & \mathbf{S}^{22} \end{bmatrix} \times \begin{bmatrix} \mathbf{P}^{\text{in},A} \\ \mathbf{P}^{\text{in},B} \end{bmatrix}, \tag{10}$$

$$\mathbf{P}^{\text{out}} = \mathbf{S} \times \mathbf{P}^{\text{in}}, \tag{11}$$

where sub-matrix $\mathbf{S}^{11}$ represents reflection of the in-going wave at port A, $\mathbf{S}^{21}$ – transmission of wave from port A to port B, $\mathbf{S}^{12}$ – the transmission of wave from port B to port A and $\mathbf{S}^{22}$ is the reflection of the in-going wave at port B.

As was mentioned in the Introduction, one step in deriving the **S**-matrix experimentally is to divide the sound pressure wave into wave propagating into the "black box" and out of it by caring out measurements at two closed duct cross sections. This procedure is possible due to the fact that both component waves will differ in phase, as can be seen from Eq. (12). The total complex amplitude of the sound pressure mode P_{mn} at the measurement cross-section z is the sum of waves travelling in both directions (cf. Eq. (12)), what according to Eq. (13) leads to the result

$$P_{ml}(z) = P_{ml}^{+} \cdot e^{-ik_{z,ml}z} + P_{ml}^{-} \cdot e^{+ik_{z,ml}z}, \tag{12}$$

$$\begin{bmatrix} P_{ml}(z) \\ P_{ml}(z+\Delta z) \end{bmatrix} = \begin{bmatrix} e^{-ik_{z,ml}z} & e^{+ik_{z,ml}z} \\ e^{-ik_{z,ml}(z+\Delta z)} & e^{+ik_{z,ml}(z+\Delta z)} \end{bmatrix} \times \begin{bmatrix} P_{ml}^{+} \\ P_{ml}^{-} \end{bmatrix}. \tag{13}$$

These measurements allow to determine the one-column matrices of $\mathbf{P}^{\text{in}}$ and $\mathbf{P}^{\text{out}}$. Note that on the left-side pipe the $P_{ml}^{\text{in}} = P_{ml}^{+}$, while on the right-side pipe $P_{ml}^{\text{in}} = P_{ml}^{-}$. As was mentioned before, the scattering matrix formalism is the most general and can be applied to an acoustic system composed of subsystems representing multi-ports of any degree (including one-ports). However, theoretical evaluation of the scattering matrix is limited to some special cases, as it requires knowledge of the reflection/transformation coefficients, R_{mln}:

$$p_{ml}^{\pm}(\rho,\varphi,z) = P_{ml}^{\pm} e^{im\varphi} \left[\frac{J_m\left(\mu_{ml}\frac{\rho}{a}\right)}{J_m\left(\mu_{ml}\right)} e^{ik_{z,ml}z} + \sum_{n=1/0}^{N_m} R_{mln} \frac{J_m\left(\mu_{mn}\frac{\rho}{a}\right)}{J_m\left(\mu_{mn}\right)} e^{-ik_{z,mn}z} \right] \tag{14}$$

(transformation of mode (ml) into mode (mn)), which were derived theoretically only for flanged (Zorumski, 1973) or unflanged (Jurkiewicz *et al.*, 2012) duct outlets.

The **S**-matrix elements can be also evaluated applying the mode matching method (MMM) and the continuity conditions together with the boundary condition at the junction (Snakowska, Jurkiewicz, 2021). However, this method requires complicated numerical calculations, and the result describes an ideal system. Thus, to determine the scattering matrix of a real system, for example – an acoustic muffler, one has to determine the **S**-matrix experimentally. As was mentioned before, the determined scattering matrix **S** will provide all necessary information about the modification of the acoustic field introduced by the system

composed of some "black boxes" connected by joints in a shape of straight pipes. If a muffler design is more complex containing irregular cavity, partition surfaces, absorption or micro-perforated elements, the scattering matrix **S** can only be determined experimentally.

4. Experimental determination of the S matrix by means of generated single modes

To experimentally determine the **S**-matrix for a muffler presented in Fig. 2 and an incident wave composed of two modes we need to excite four independent sound fields and proceed measurements according to the method described previously.

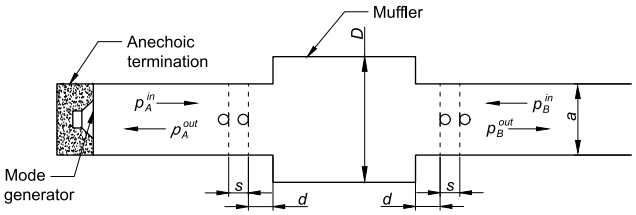

Fig. 2. Sketch of the measuring set-up.

In general, the sound pressure at each port consists of the in-going and out-going wave (Lee *et al.*, 2020). In the case of a perfect anechoic termination, there will be no wave incoming to the muffler on the side B, so $p_B^{\text{in}} = 0$.

However, because of the symmetry of the muffler we can limit ourselves to generation of two fields. Note that measurement data for a given field allow to determine only N of the **S**-matrix elements and that generation of pure one-mode fields ((0,0) and (0,1)) with ideal anechoic termination at the outlet pipe leads to the result

$$\mathbf{P}_{\text{in}} = \begin{bmatrix} 1 & 0 & 0 & 0 \\ 0 & 1 & 0 & 0 \\ 0 & 0 & 1 & 0 \\ 0 & 0 & 0 & 1 \end{bmatrix} \rightarrow \mathbf{S} = \mathbf{P}_{\text{out}}. \tag{15}$$

Thus, it is obvious that generating independent sound fields with a single-mode generator greatly simplifies the calculation procedure, however their generation is complicated and moreover requires special equipment. In theory, the selected mode should be generated as a single one and should not be accompanied by other propagating modes. In this case, the matrix of the incoming pressure wave measurement data is either a diagonal or a unit matrix (if the data is properly normalized).

Generating a single mode by means of the mode synthesizer (Snakowska *et al.*, 2016) (cf. Fig. 3a) requires precise determination of the relative amplitudes and phases of individual point sources, which are sensitive to any inaccuracies, and the experimental error increases with the difference between the excitation frequency and the cut-off frequency of the generated mode. More details can be found in (Snakowska *et al.*, 2016). The single-mode generation method based on Green's function is particularly sensitive to the correct positioning of the point source in the grid node of the source matrix (cf. Fig. 3a). The eccentricity of the measuring grid (microphone positioning), as well as of point sources, was found to be another possible source of error (Snakowska *et al.*, 2016). The parameters of the muffler are as follows: inlet/outlet pipe of radius a = 103.2 mm, for which cut-on frequency of the first higher order mode (1,1) is 976 Hz (ka = 1.84). The radius of the expansion chamber is 183.2 mm. The length of the expansion chamber is 444 mm. The distance between the measurement planes Δz to decompose the wave into ingoing and out-going wave is 60 mm. At the end of the inlet pipe the mode synthesizer is mounted. For the excitation frequency 2122 Hz (ka = 4) four modes are cut-on modes, of which first axisymmetrical mode (0,1) is fourth in the order of occurrence considering the cut-on frequency and so it has index 4. To reduce the experimental error, the data were taken from a grid of points formed by the movement of microphones along the duct radius with a resolution of 5 mm. The set of

a)

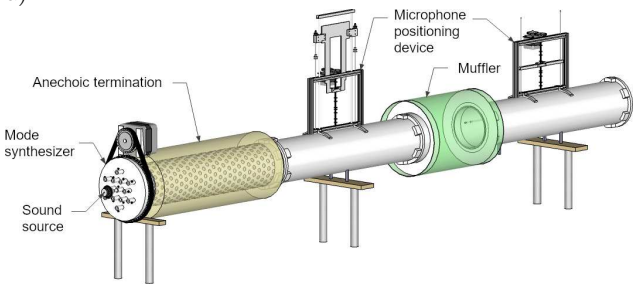

b)

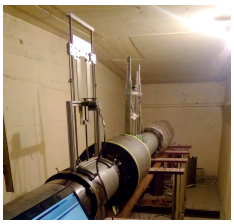

c)

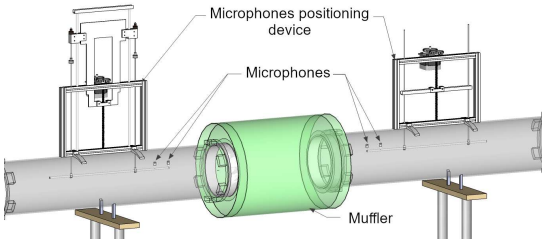

Fig. 3. a) visualization of the measurement set-up, b) picture of the real measurement set-up, c) sketch of the microphones positioning device.

point sources was rotated in the range of 360° with an angular resolution of 15° (Fig. 3). Combination of these two motions results in the possibility to scan the duct cross-section with resolution of 15° in the azimuthal angle and 5 mm in the diameter.

A monochrome measurement signal was generated. The frequency was chosen in such way that the generated frequency is halfway between the cut-on frequencies of the highest cut-on mode and the first cut-off mode (Fig. 4).

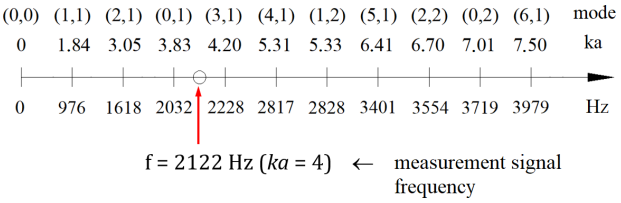

Fig. 4. Selection of the excitation frequency.

The complex amplitudes of individual point sources of the source matrix allowing to generate a single mode were determined on the basis of the duct-Green's function (Snakowska *et al.*, 2016)

$$G(\mathbf{r},\mathbf{r}') = \frac{-i}{2\pi a^2}\sum_{m,l}\frac{J_m\left(\mu_{ml}\frac{\rho}{a}\right)J_m\left(\mu_{ml}\frac{\rho'}{a}\right)}{\left(1-\frac{m^2}{\mu_{ml}^2}\right)J_m^2\left(\mu_{ml}\right)k_{z,ml}} \cdot e^{-ik_{z,ml}(z-z')-im(\varphi-\varphi')}. \tag{16}$$

The measurement data together with distribution of point sources at the mode synthesizer are presented in Table 1.

Table 1. Modules of relative amplitudes and phases of the excitation signals supplied to individual sources.

Source	Mode (0,0)		Mode (0,1)		Arrangement of the point sound sources in a mode synthesizer
	Amp. [%]	Phase [rad]	Amp. [%]	Phase [rad]	
1	46	0	46	π	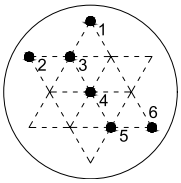
2	46	0	46	π	
3	100	π	100	0	
4	57	0	3	0	
5	10	0	10	π	
6	0	0	0	0	

The measurements were carried out on both sides of the muffler in two planes of the cross-section of the inlet and outlet pipe to separate the in-going and outgoing waves. As the muffler is symmetrical, it was possible to supplemented the next two rows of the $\mathbf{P}^{\text{in}}$, $\mathbf{P}^{\text{out}}$ matrices with the same measurement results. The **S**-matrix technique requires use of four microphones simultaneously and the synchronization of their mutual positioning with respect to the axis of the system. The microphones were mounted in pairs on both sides of the muffler on measuring arms, the positioning of which was determined by two stepper motors of the same type. The control signal of both motors was generated from a common controller, which allowed synchronization of the position of the microphones.

5. Results

Figures 5 and 6 show the distribution of the sound pressure level obtained experimentally. Shape and am-

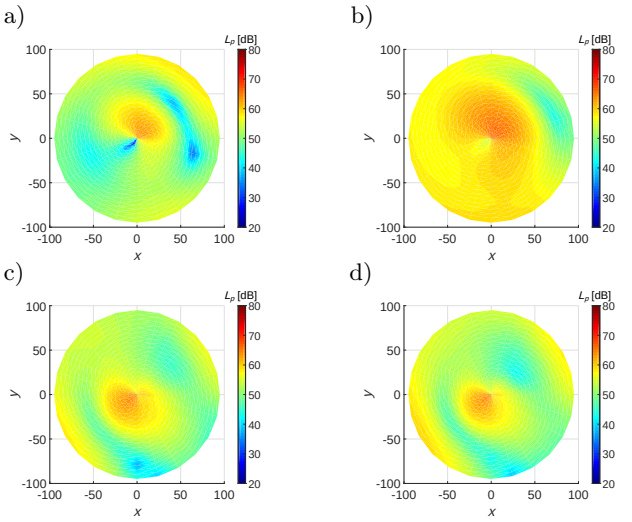

Fig. 5. Distribution of mode (0,0) sound pressure level (for the generation of the mode (0,0) according to the amplitudes and phases from Table 1): a), b) in two planes of the cross-section of pipes connected to the muffler – side A, c), d) in two planes of the cross-section of pipes connected to the muffler – side B.

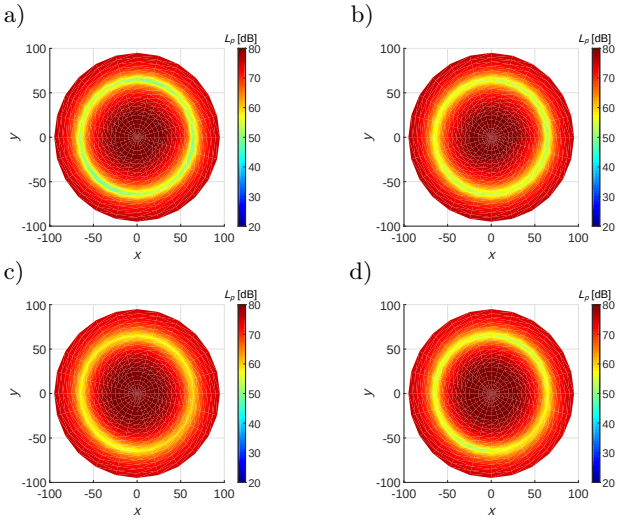

Fig. 6. Distribution of mode (0,1) sound pressure level (for the generation of the mode (0,1) according to the amplitudes and phases from Table 1): a), b) in two planes of the cross-section of pipes connected to the muffler – side A, c), d) in two planes of the cross-section of pipes connected to the muffler – side B.

plitude of the waves can be observed on both sides of the muffler (A side and B side).

The results of the mode decomposition are shown in Fig. 7. The mode of index 4 (axial (0,1) mode) significantly dominates, so it can be assumed that the incident wave is in the form of a single mode (Fig. 7b). In practice, excitation of the field in the form of a single mode is rather difficult, especially when the cut-off frequency of the generated mode is far from the excitation frequency – Fig. 7a.

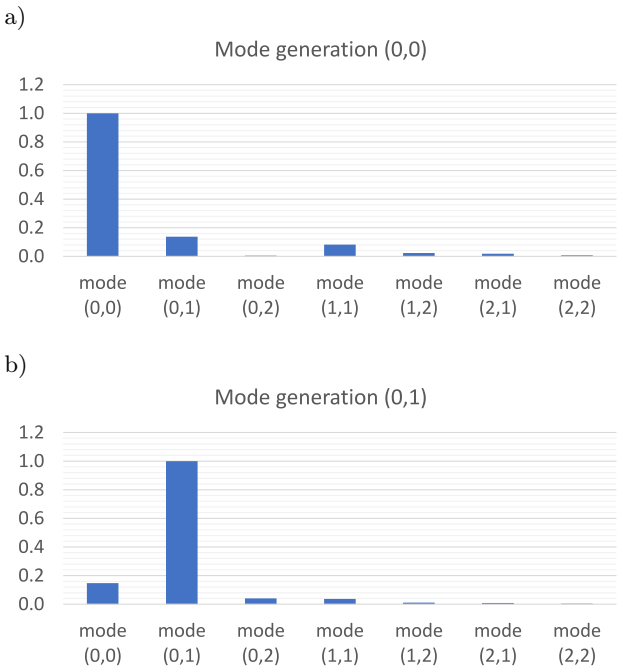

Fig. 7. Mode decomposition – normalized amplitude of the modes wave: a) mode (0,0) for the generation of the single mode (0,0), b) mode (0,1) for the generation of the single mode (0,1).

The obtained mode amplitudes after decomposition (for each of the four waves) were normalized to the value 1, which means the highest occurring value of the mode amplitude (0,1). In further considerations the presence of circumferential modes (1,1) and (2,1) was neglected and so $\mathbf{P}^{\text{in}}$ and $\mathbf{P}^{\text{out}}$ matrices, on the basis of which the scattering matrix was calculated according to formula Eq. (17), are of the 4×4 dimension. In theory, scattering matrix of single mode field is diagonal. In the analysed case, we obtained the matrices presented below

$$\begin{aligned} \mathbf{P}_{\text{in}} &= [\mathbf{P}_{\text{in1}} \quad \mathbf{P}_{\text{in2}} \quad \mathbf{P}_{\text{in3}} \quad \mathbf{P}_{\text{in4}}], \\ \mathbf{P}_{\text{out}} &= [\mathbf{P}_{\text{out1}} \quad \mathbf{P}_{\text{out2}} \quad \mathbf{P}_{\text{out3}} \quad \mathbf{P}_{\text{out4}}], \\ \mathbf{S} &= \mathbf{P}_{\text{out}} \times \mathbf{P}_{\text{in}}^{-1}, \\ \mathbf{S} &= [\mathbf{S}_1 \quad \mathbf{S}_2 \quad \mathbf{S}_3 \quad \mathbf{S}_4], \end{aligned} \tag{17}$$

where

$$\mathbf{P}_{\text{in1}} = \begin{bmatrix} 1 \\ 0.113 - 0.079i \\ 0.085 - 0.248i \\ 0.165 + 0.017i \end{bmatrix}, \quad \mathbf{P}_{\text{in2}} = \begin{bmatrix} -0.066 - 0.126i \\ 1 \\ -0.179 - 0.113i \\ -0.782 + 0.461i \end{bmatrix},$$

$$\mathbf{P}_{\text{in3}} = \begin{bmatrix} 0.085 - 0.248i \\ 0.165 + 0.017i \\ 1 \\ 0.113 - 0.079i \end{bmatrix}, \quad \mathbf{P}_{\text{in4}} = \begin{bmatrix} -0.179 - 0.113i \\ -0.782 + 0.461i \\ -0.066 - 0.126i \\ 1 \end{bmatrix},$$

$$\mathbf{P}_{\text{out1}} = \begin{bmatrix} 0.924 + 0.336i \\ 0.137 + 0.021i \\ -0.092 - 0.263i \\ -0.154 + 0.072i \end{bmatrix}, \quad \mathbf{P}_{\text{out2}} = \begin{bmatrix} -0.025 - 0.153i \\ 0.713 + 0.668i \\ -0.025 - 0.153i \\ 0.441 - 0.808i \end{bmatrix},$$

$$\mathbf{P}_{\text{out3}} = \begin{bmatrix} -0.092 - 0.263i \\ -0.154 + 0.072i \\ 0.924 + 0.336i \\ 0.137 + 0.021i \end{bmatrix}, \quad \mathbf{P}_{\text{out4}} = \begin{bmatrix} -0.025 - 0.153i \\ 0.441 - 0.808i \\ -0.025 - 0.153i \\ 0.713 + 0.668i \end{bmatrix},$$

$$\mathbf{S}_1 = \begin{bmatrix} 0.964 + 0.297i \\ -0.004 + 0.229i \\ -0.235 - 0.024i \\ -0.212 + 0.304i \end{bmatrix}, \quad \mathbf{S}_2 = \begin{bmatrix} -0.067 - 0.098i \\ 0.316 - 0.480i \\ 0.003 - 0.068i \\ 0.387 - 1.296i \end{bmatrix},$$

$$\mathbf{S}_3 = \begin{bmatrix} -0.235 - 0.024i \\ -0.212 + 0.304i \\ 0.964 + 0.297i \\ -0.004 + 0.229i \end{bmatrix}, \quad \mathbf{S}_4 = \begin{bmatrix} 0.003 - 0.068i \\ 0.387 - 1.296i \\ -0.067 - 0.098i \\ 0.316 - 0.480i \end{bmatrix}.$$

The presented example clearly shows the advantages of using a single mode generator to determine the effectiveness of reflective muffler using the scattering matrix formalism.

Based on the determined $\mathbf{P}_{\text{in}}$ and $\mathbf{P}_{\text{out}}$ matrices, calculations of the average acoustic power value of the sum of the modes (0,0) and (0,1) were carried out according to the Eq. (18)

$$W = \frac{1}{2}\pi a^2 \rho_0 c k \left[\sum_{m=0} \sum_{n=1} k_{z,ml} \left| A_{ml}^2 \right|^2 \cdot \left(1 - \frac{m^2}{\mu_{ml}^2} \right) + k \left| A_{00} \right|^2 \right], \tag{18}$$

where ρ_0 – medium density, $k_{z,ml} = \frac{1}{a}\sqrt{(ka)^2 - \mu_{ml}^2}$ – axial wave number, A_{ml} – amplitude of modes, m – circumferential mode index (in this case $m = 0$), A_{00} – amplitude of mode (0,0), μ_{ml} – n-th root of the Bessel function $J_m^{'}(\cdot)$.

The calculated values of acoustic power were used to determine the transmission loss TL parameter of the muffler attenuation presented in Eq. (19)

$$\text{TL} = 10 \log \left| \frac{W_i}{W_t} \right|, \tag{19}$$

where W_i – acoustic power of incident wave, W_t – acoustic power of transmitted wave.

For the generation of a wave in the form of a plane wave (single mode (0,0)) taking into account presence of mode (0.1) in the generated sound field also, the acoustic power ratio of the incident and transmitted wave is W_i/W_t = 11.61 and TL = 10.64 dB. For generation single mode (0,1) taking into account also presence of mode (0,0) the value is W_i/W_t = 1.14 and TL = 0.6 dB. Table 2 presents also these values considering only single mode in the excited field.

Table 2. Values of transmission loss of investigated reflective muffler.

	Generation mode (0,0)		Generation mode (0,1)	
	modes (0,0) + (0,1)	mode (0,0)	modes (0,0) + (0,1)	mode (0,1)
W_i/W_t	11.61	12.78	1.14	1.17
TL [dB]	10.64	11.06	0.60	0.71

Analysing results of the effectiveness on the sound level lowering, it can be seen that the investigated muffler is quite effective for the plane wave (mode (0,0)) as the TL is above 10 dB. However, it is not effective for the incident wave in the form of a single mode (0,1) when the TL is less that one decibel. In the literature, results of the attenuation effectiveness of mufflers are usually presented for frequencies below the cut-off frequency of higher order modes or a multimode wave composed of many modes (including plane wave). For this reason, it is hard to compare experimental results of the attenuation efficiency of the reflective muffler for an acoustic wave in the form of a single higher mode. It may be caused by the geometrical dimensions of the expansion chamber of the reflective muffler. The attenuation efficiency of a reflective muffler for the higher single-mode excitation should be confirmed in future studies.

6. Conclusions

The main steps of the applied method, experimental results allowing to determine the scattering matrix of example muffler and results for the investigated one can be summarised as follows:

- The applied methods of multi-port and scattering matrix are fairly general and can be applied to many duct-like acoustic system including mufflers of complex design.
- Determination of the **S**-matrix is an inverse problem and requires the experimental data matrix to be well determined.
- Propagation of an N-mode wave through the system requires excitation and measurements of $2N$ different sound fields.
- Excitation of these fields in form of consecutive single modes by means of single mode generator assures the exited fields to be substantially different what in turn minimises the final results error.
- Measurements of the acoustic pressure inside a rigid cylindrical waveguide on both sides of the muffler were performed in two planes of the inlet/outlet pipe cross-section spaced from each other by 60 mm. Mode decomposition was performed for each of the four measurement planes to determine the amplitude of each mode.
- The waves on both sides of the muffler were separated into in-going and out-going waves from the muffler. The obtained amplitudes were normalized and their values were used to determine the scattering matrix **S** of the reflective muffler.
- The scattering matrix determines the attenuation parameters of the acoustic muffler thoroughly. Based on the scattering matrix **S** coefficients, the muffler effectiveness was determined as the transmission loss (TL) parameter. The calculations confirmed the effectiveness of the muffler for the incident acoustic wave in the form of a single mode (0,0). In the case of mode (0,1), the muffler is ineffective.

Acknowledgments

The study reported in this paper was financed by the Dean's of the Faculty of Mechanical Engineering and Robotics AGH University of Science and Technology – research project number 16.16.130.942.

References

1. Åbom M. (1991), Measurement of the scattering-matrix of acoustical two-ports, *Mechanical System and Signal Processing*, **5**(2): 89–104, doi: 10.1016/0888-3270(91)90017-Y.
2. Åbom M., Karlsson M. (2010), Can acoustic multiport models be used to predict whistling, *16th AIAA/CEAS Aeroacoustics Conference*, **5**: 4285–4292.
3. Atig M., Dalmont J.P., Gilbert J. (2004), Termination of open-end cylindrical tubes at high sound pressure level, *Computes Rendus Mecanique*, **332**(4): 299–304, doi: 10.1016/j.crme.2004.02.008.
4. Auger J.M., Ville J.M. (1990), Measurement of linear impedance based on the determination of duct eigenvalues by a Fourier-Lommel's transform, *The Journal of the Acoustical Society of America*, **88**(1): 19–22, doi: 10.1121/1.399942.
5. Auregan Y., Farooqui M., Groby J.P. (2016), Low frequency sound attenuation in a flow duct using a thin slow sound material, *The Journal of the Acoustical Society of America*, **139**(5): 149–153, doi: 10.1121/1.4951028.
6. Chen X.X., Zhang X., Morfey C.L., Nelson P.A. (2004), A numerical method for computation of sound radiation from an unflanged duct, *Journal*

of Sound and Vibration, **270**(3): 573–586, doi: 10.1016/j.jsv.2003.09.055.

7. Dalmont J.P., Nederveen C.J., Joly N. (2001), Radiation impedance of tubes with different flanges: numerical and experimental investigations, *Journal of Sound and Vibration*, **244**(3): 505–534, doi: 10.1006/jsvi.2000.3487.
8. Gerges S.N.Y., Jordan R., Thieme F.A., Bento Coelho J.L., Arenas J.P. (2005), Muffler modeling by transfer matrix method and experimental verification, *Journal of the Brazilian Society of Mechanical Sciences and Engineering*, **27**(2): 132–140, doi: 10.1590/S1678-58782005000200005.
9. Hocter S.T. (1999), Exact and approximate directivity patterns of the sound radiated from a cylindrical duct, *Journal of Sound and Vibration*, **227**(2): 397–407, doi: 10.1006/jsvi.1999.2351.
10. Hocter S.T. (2000), Sound radiated from a cylindrical duct with Keller's geometrical theory, *Journal of Sound and Vibration*, **231**(5): 1243–1256, doi: 10.1006/jsvi.1999.2739.
11. Joseph P., Morfey C.L. (1999), Multimode radiation from an unflanged, semi-infinite circular duct, *The Journal of the Acoustical Society of America*, **105**(5): 2590–2600, doi: 10.1121/1.426875.
12. Jurkiewicz J., Snakowska A., Gorazd Ł. (2012), Experimental verification of the theoretical model of sound radiation from an unflanged duct with low mean flow, *Archives of Acoustics*, **37**(2): 227–236, doi: 10.2478/v10168-012-0030-7.
13. Lavrentjev J., Abom M., Boden H. (1995), A measurement method for determining the source data of acoustic two-port sources, *Journal of Sound and Vibration*, **183**(3): 517–531, doi: 10.1006/jsvi.1995.0268.
14. Lee J.K., Oh K.S., Lee J.W. (2020), Methods for evaluating in-duct noise attenuation performance in a muffler design problem, *Journal of Sound and Vibration*, **464**: 114982, doi: 10.1016/j.jsv.2019.114982.
15. Lidoine S., Batard H., Troyes S., Delnevo A., Roger M. (2001), Acoustic radiation modelling of aeroengine intake comparison between analytical and numerical methods, *7th AIAA/CEAS Aeroacoustics Conference and Exhibit*, Maastricht, doi: 10.2514/6.2001-2140.
16. Munjal M.L. (1987), *Acoustics of Ducts and Mufflers with Application to Exhaust and Ventilation System Design*, New York: John Wiley & Sons.
17. Sack S., Abom M., Efraimsson G. (2016), On acoustic multi-port characterisation including higher order modes, *Acta Acustica United with Acustica*, **102**(5): 834–850, doi: 10.3813/AAA.918998.
18. Selamet A., Dickey N.S., Novak J.M. (1994), The Herschel-Quincke tube: A theoretical, computational, and experimental investigation, *The Journal of the Acoustical Society of America*, **96**(5): 3177–3185, doi: 10.1121/1.411255.
19. Sinayoko S., Joseph P., McAlpine A. (2010), Multimode radiation from an unflanged, semi-infinite circular duct with uniform flow, *The Journal of the Acoustical Society of America*, **127**(4): 2159–2168, doi: 10.1121/1.3327814.
20. Sitel A., Ville J.M., Foucart F. (2006), Multiload procedure to measure the acoustic scattering matrix of a duct discontinuity for higher order mode propagation conditions, *The Journal of the Acoustical Society of America*, **120**(5): 2478–2490, doi: 10.1121/1.2354040.
21. Snakowska A., Gorazd Ł., Jurkiewicz J., Kolber K. (2016), Generation of a single cylindrical duct mode using a mode synthesizer, *Applied Acoustics*, **114**: 56–70, doi: 10.1016/j.apacoust.2016.07.007.
22. Snakowska A., Jurkiewicz J. (2010), Efficiency of energy radiation from an unflanged cylindrical duct in case of multimode excitation, *Acta Acustica united with Acustica*, **96**(3): 416–424, doi: 10.3813/AAA.918294.
23. Snakowska A., Jurkiewicz J. (2021), A new approach to the theory of acoustic multi-port networks with multimode wave and its application to muffler analysis, *Journal of Sound and Vibration*, **490**: 115722, doi: 10.1016/j.jsv.2020.115722.
24. Snakowska A., Jurkiewicz J., Gorazd Ł. (2017), A hybrid method for determination of the acoustic impedance of an unflanged cylindrical duct for multimode wave, *Journal of Sound and Vibration*, **396**: 325–339, doi: 10.1016/j.jsv.2017.02.040.
25. Song B. H., Bolton J.S. (2000), A transfer-matrix approach for estimating the characteristic impedance and wave numbers of limp and rigid porous materials, *The Journal of the Acoustical Society of America*, **107**(3): 1131–1152, doi: 10.1121/1.428404.
26. Su J., Rupp J., Garmory A., Carrotte J.F. (2015), Measurements and computational fluid dynamics predictions of the acoustic impedance of orifices, *Journal of Sound and Vibration*, **352**: 174–191, doi: 10.1016/j.jsv.2015.05.009.
27. Zorumski W.E. (1973), Generalized radiation impedances and reflection coefficients of circular and annular ducts, *The Journal of the Acoustical Society of America*, **54**(6): 1667–1673, doi: 10.1121/1.1914466.